Flipping Photons Backward: Reversed Cherenkov Radiation Inspired by Metamaterials

Hongsheng Chen,[1,2*] Min Chen[3†]

Charged particles traveling through a conventional medium at a speed greater than the speed of light in the medium produce Cherenkov radiation in the forward directions, which is useful for particle identification and counting. Newly designed metamaterial, with their negative index of refraction, flips the radiated photons backward and thus readily separates the radiation from the emitting particles, providing high flexibility in the manipulation of the photons. Here we review the recent advances in reversed Cherenkov radiation research and discuss the potential that metamaterial may hold for developing new types of devices.

Introduction

While matter cannot be accelerated beyond the speed of light in vacuum, light may propagate significantly slower in a dielectric medium and matter can exceed light in speed under some circumstances. When a charged particle travels through a dielectric medium with a speed greater than the speed of light in the same medium, electromagnetic radiation or photons are emitted by the medium under the action of the field of the particle moving in it. This phenomenon, known as Cherenkov radiation, was first observed by Cherenkov (*1*) and theoretically interpreted by Tamm and Frank (*2*). Since the energy and angle of the emitted Cherenkov radiation depend on the speed of the charged particles, these characteristics can be used to detect and count the particles. Such device called as Cherenkov counters has made many prominent discoveries in Particle Physics possible, including the antiproton (*3*) and the J particle (*4*). Nowadays Cherenkov radiation has been widely used in experiments for identifying fast particles, measuring the intensity of reactions, detecting the labeled biomolecules, and determining the source and intensity of the cosmic rays, etc.

In a conventional dielectric medium, Cherenkov radiation possesses three key characteristics: 1) electromagnetic waves are radiated only if the velocity of the charge is larger than the phase velocity of light in the medium, 2) the constant phase front of the radiated wave forms a cone and propagates forward, and 3) the polarization of the electric field vector lies in the plane determined by the velocity vector of charge and the direction vector of the wave radiation, i.e. transverse magnetic field (TM). Since Cherenkov radiation travels in the same direction as that of the particles, the charged particle will interfere with the detection of the forward radiated photons. It can be difficult to shield the Cherenkov detector from radiation damage and to extract the useful radiation from the noise of the high-energy particles.

The abnormal reversed Cherenkov radiation in the left-handed medium (LHMs) with simul-

taneously negative permittivity and negative permeability allows the backward emitted wave to be easily separable from the high energy particles. In the left-handed medium, the electric field $\overline{E}$, magnetic field $\overline{H}$, and wave vector $\overline{k}$ form a left-handed trial, yielding a backward wave propagation – the phase propagation direction represented by the wave vector is opposite to the energy flow (*5*). This is in contrast to the wave propagation in the conventional medium, where $\overline{E}$, $\overline{H}$, and $\overline{k}$ form a right-handed triad. The conventional medium is thus also called as right-handed medium (RHM). Because the wave undergoes a negative phase when propagating forward in the left-handed medium, the phase refractive index of the left-handed medium is negative. From one point of view, the left-handed medium can be equivalently treated as a negative space medium (*6*), when a charged particle moving forward in the left-handed medium, it looks like moving in the opposite direction in a conventional medium and radiates wave forward. From another point of view, the left-handed medium also can be treated as a time reversal medium (*7*), the backward wave radiated from the fast moving charged particle looks as if the phase front of the wave chases toward the particle, instead of spreads out from the particle. Such unusual medium can be realized by a collection of some artificial resonant elements whose size and spacing are much smaller than the wavelength of concern. These artificial elements play the similar roles as atoms or molecules and a collection of these artificial elements give an macroscopic electromagnetic response characterized by negative permittivity and negative permeability. Such artificial material with unusual properties is called as metamaterial, which offers some novel electromagnetic properties that are not found in nature (*8*). The use of metamaterial can enables us to exploit some exotic phenomena associated with Cherenkov radiation and open a new window of novel applications in High-Energy Physics, Astrophysics, and Biology, etc.

Here we provide an overview of the applications of the metamaterials in Cherenkov radiations, examine how to achieve the reversed Cherenkov radiation, and discuss the design

principles of metamaterials for reversed Cherenkov radiation. The issue of how energy and momentum conserve is also discussed. We conclude by highlighting the practical potential of this field and the challenging work remains to be solved in order to realize that potential.

Physical Origin of Cherenkov Radiation

Fig. 1(a) illustrates how a fast charged particle generates a forward Cherenkov radiation cone in a conventional material with a positive refractive index of n. We assume the particle travels along the z direction with a speed of v. At $t = t_0$, t_1, t_2, and t_3, it moves to position 0, 1, 2, and 3, respectively. At $t = t_0$, the particle travels at position 0 and drive the medium to radiate a spherical wave spread from position 0. At $t = t_1$, the phase front of the radiated wave represented by the circle travels a distance of ct_1/n (c is the speed of light in vacuum) but the particle has already travels a distance of vt_1 reaching position 1 where another spherical wave start to be radiated. As time passes, the particle travels further, new spherical waves will be radiated out and the former radiated outgoing spherical waves also spread out further from their individual centers. The phase fronts of the spherical waves in phase with one another are marked in the same color as shown in Fig. 1(a). It is obvious that the envelope of these spherical waves in the same color forms a conic wave front. If we define θ to be the angle between the direction of motion of the particle and the direction of the radiated shock wave, we find that $\theta = \cos^{-1}[c/(nv)]$. The direction of the shock wave therefore forms a forward Cherenkov radiation cone with an angle of 2θ.

In a left-handed medium with negative refractive index, similar illustration is presented in Fig. 1(b). As the particle travels along the z direction, the emitted wave has the energy flowing outward. However, since the phase refractive index is negative, the phase (represented by the circles) becomes more negative as the waves radiated out further from their individual centers. The phase fronts of the spherical waves therefore do not spread outward from their individual

centers, but instead converge towards them as time passed. Different from that in right-handed medium, we see the in-phased circles increase from position 0 to position 3 as the particle travels from position 0 at $t = t_0$ to position 3 at $t = t_3$, yielding a set of planar wavefronts traveling toward the trajectory of the particle. The cone of the energy flow will be directed backward related to the motion of the particle. The angle of the cone, $\theta = \cos^{-1}[c/(nv)]$, is hence obtuse for $n < -1$.

In fact, in our daily life we often encounter some phenomena similar to Cherenkov radiation. For example, the wake water waves form a shock front behind the boat when it travels faster than the speed of water wave, and the sonic booms can be heard when an aircraft moves faster than the speed of sound. Similarly, the charged particle produces Cherenkov radiation only when it exceed the speed of light in the medium. We know the wave vector and frequency of an electromagnetic wave propagated in a dielectric medium are related by $k = n\omega/c$. Considering the similarity of the photon and a fast charged particle, the frequency of the Fourier component of the field of a moving particle is related to the z-component of the wave vector by $\omega = k'_z v$, which should be consistent with the z-component of the radiated wave k_z because the radiated wave is associated with the fast moving particle. Since $k > k_z = k'_z$, we get a threshold of the velocity of particle: $v > c/n$. Therefore only when the velocity of the particle exceeds the phase velocity of waves in the medium, electromagnetic waves can be radiated. When the velocity of the particle is smaller than the threshold, the wave will be evanescent in the far field region.

Theoretical considerations: how is energy-momentum conserved in a reversed Cherenkov radiation

A charged particle loses energy in emitting Cherenkov radiation, and slows down. While the energy transfer in the Cherenkov radiation can be easily understood, the momentum trans-

fer from the particle to the radiated waves is rather complicated. This is because the definition of electromagnetic wave momentum in left-handed medium is not straightforward. The popular simple definition of the time averaged wave momentum in Minkowski form, $\langle\overline{G}\rangle = \frac{1}{2}\mathbf{Re}\{\overline{D}\times\overline{B}^*\}$ (*9–11*), does not hold in the left-handed medium. Consider the simplest case of an isotropic left-handed medium with ϵ and μ, this definition leads to the wave momentum $\langle\overline{G}\rangle = \frac{1}{2}\mathbf{Re}\{\epsilon\mu^*\overline{E}\times\overline{H}^*\}$ in the same direction as the energy flow defined by the Poynting vector $\langle\overline{S}\rangle = \frac{1}{2}\mathbf{Re}\{\overline{E}\times\overline{H}^*\}$ since both ϵ and μ are negative. It would imply the emitting charged particle would gain momentum and thus energy while emitting Cherenkov wave in the backward direction (*12*), obviously violating the conservation of energy and also the third fundamental law of thermodynamics, which stipulates that charged particles radiate energy and therefore lose energy. If loss is very small and can be neglected, $\overline{k}$ is real, we use the following classical form to define the wave momentum density in a dispersive left-handed medium: $\langle\overline{G}\rangle = \frac{1}{2}\mathbf{Re}\{\overline{D}\times\overline{B}^* + \frac{\overline{k}}{2}(\frac{\partial\bar{\epsilon}}{\partial\omega}\overline{E}\cdot\overline{E}^* + \frac{\partial\bar{\mu}}{\partial\omega}\overline{H}\cdot\overline{H}^*)\}$, which contains the Minkowski momentum $\overline{D}\times\overline{B}^*$ plus material dispersion terms (*13*). For isotropic left-handed medium, the average momentum density reduces to the momentum given by Veselago (*5*). By noting that $\mathbf{Re}\{\overline{D}\times\overline{B}^*\} = \mathbf{Re}\{\overline{D}\times(\frac{\overline{k}}{\omega}\times\overline{E})^*\} = \mathbf{Re}\{\frac{\overline{k}}{\omega}(\overline{D}\cdot\overline{E}^*)\} = \mathbf{Re}\{\frac{\overline{k}}{\omega}(\overline{B}\cdot\overline{H}^*)\}$, and noting that the electromagnetic field energy for dispersive medium is defined as $W = \frac{1}{4}(\frac{\partial(\omega\bar{\epsilon})}{\partial\omega}\overline{E}\cdot\overline{E}^* + \frac{\partial(\omega\bar{\mu})}{\partial\omega}\overline{H}\cdot\overline{H}^*)$, we can get $\langle\overline{G}\rangle = \frac{1}{4}\mathbf{Re}\{\frac{\overline{k}}{\omega}\left[(\bar{\epsilon}+\omega\frac{\partial\bar{\epsilon}}{\partial\omega})\overline{E}\cdot\overline{E}^* + (\bar{\mu}+\omega\frac{\partial\bar{\mu}}{\partial\omega})\overline{H}\cdot\overline{H}^*\right]\} = \frac{W}{\omega}\overline{k}$. We therefore see that the momentum vector is along the $\overline{k}$ direction. This statement is in agreement with the Quantum Physics argument, where the wave momentum in medium follows the Abraham's form $\langle\overline{G}\rangle = \hbar\overline{k}$, where $\hbar = \frac{W}{\omega}$ is the reduced Plank's constant (*14*). The time averaged Poynting vector $\langle\overline{S}\rangle = \langle\overline{E}\times\overline{H}^*\rangle = \langle\overline{E}\times\frac{1}{\omega\mu^*}(\overline{k}\times\overline{E})^*\rangle = \langle\frac{1}{\omega\mu^*}\overline{k}^*|E|^2\rangle = \frac{|E|^2}{2\omega\mu}\overline{k}$ is opposite to the wave vector for negative μ, representing a backward propagating wave. We therefore see that in isotropic left-handed medium, the momentum of the Cherenkov radiated wave is forward, which is directed opposite to the direction of the energy flow. The momentum and energy are

thus both conserved. When loss cannot be neglected, a classical definition of the momentum vector has been addressed in (*13*). It has been pointed out that in isotropic left-handed medium when the loss is increased, the momentum density $\langle\overline{G}\rangle$ may be parallel to the power flow (*15*). This is because the material dispersion terms in the expression of $\langle\overline{G}\rangle$ becomes minor compared with the first term represented by Minkowski momentum. However, momentum conservation law is still valid because a recoiled force $\langle\overline{f}\rangle = -\frac{1}{2}\mathbf{Re}\{\omega\epsilon_I\overline{E}\times\overline{B}^* - \omega\mu_I\overline{H}\times\overline{D}^*\}$ opposed by the medium will be raised as the wave attenuates in the lossy medium (*15*).

Metamaterial design for Reversed Cherenkov Radiation

To successfully test the reversed Cherenkov radiation, the following three issues must be addressed: 1) the design of a suitable isotropic left-handed medium, 2) an efficient Cherenkov radiation source equivalent to fast charged particles, and 3) a detector to clearly demonstrate the backward radiated waves.

We first discuss the design of a suitable isotropic left-handed medium. μ and ϵ in general are 3×3 matrices. For the simple case of a charged particle moving and accelerated in the z-direction in a cylindrical coordinate system, the magnetic field is non-zero only along the ϕ direction and the electric field only along the ρ and the z directions. Due to this symmetry, the only relevant components are the $\hat{\phi}\hat{\phi}$ component for μ and the two orthogonal components $\hat{\rho}\hat{\rho}$ and $\hat{z}\hat{z}$ for ϵ.

The fundamental elements for the realization of left-handed medium was already proposed by Pendry and his colleagues about a decade ago. One is a periodic arrangement of thin metal wires, which can exhibit a negative permittivity for certain frequencies (*16*), and the other is split-ring resonators that, correspondingly, exhibit a negative permeability for certain frequencies (*17*). The combined structure of these two fundamental elements has been realized in 2000 (*18*) and the negative index of refraction of the left-handed medium predicted by Veselago

has been confirmed (*19*). Lots of more metamaterial designs have been proposed later by different arrangement of these fundamental elements or some evolved resonant elements. However, most of them were designed for electromagnetic wave with out-of-plane electric field (TE) and are not suitable for testing reversed Cherenkov radiation, which is transverse magnetic (TM) field.

A new type of left-handed metamaterial has been experimentally fabricated for the detection of Cherenkov radiation recently (*20*). A slide in the ϕ direction of the metamaterial composed of many substrate layers repeated along the y (or the ϕ) direction with each layer printed with split-ring resonators and metal wires, is shown in Fig. 2(a). In each layer, the orthogonal copper wires are printed on both sides of the thin dielectric sheet providing isotropic negative permittivity in the xz plane, while the two L-shaped metal strips on the top side coupled with the two on the bottom side to form an equivalent inductor/capacitor *LC* resonator, providing a negative permeability response along the y direction.

The effective permeability of the L-shaped split-ring resonators can be derived following the method proposed in (*17, 21*). Consider the response of a stack of rings to an incident electromagnetic wave with magnetic field polarized along the y direction. A column of the split-ring resonators behaves like a solenoid. The oscillating incident magnetic field induces circumferential surface currents which tend to generate a magnetization opposing the applied field, as a consequence of Lenz's law. If we assume $\hat{y}H_0$ to be the incident magnetic field and J to be the induced current per unit length around the loop, then the amplitude of the magnetic fields (along the $\hat{y}$ direction) inside and outside of the loop will be $H_{int} = H_0 + J - FJ$, and $H_{ext} = H_0 - FJ$, where F is the fractional area of the periodic unit cell in the xz plane occupied by the interior of the split-ring resonator. The above two fields are calculated from the Ampere's law which gives $H_{ext} - H_{int} = -J$, and the magnetic flux equation which gives $B_{ave} = \mu_0 F H_{int} + \mu_0(1-F)H_{ext} = \mu_0 H_0$. Note that

we are realizing artificial magnetic 'molecular', the field inside of the 'molecular' is of little interest as the macroscopic parameters are dependent on the field outside of the 'molecular'. The average magnetic field density is therefore defined as $H_{ave} = H_{ext}$. The effective permeability is defined as $\mu_{eff} = B_{ave}/H_{ave} = \mu_0 H_0/(H_0 - FJ)$. The induced current can be calculated by using Faraday's law, from which we get, $emf = \oint d\bar{l} \cdot \overline{E} = 4lE_1 + 4tE_2 = -\frac{d}{dt}\int\int d\bar{s} \cdot \mu_0 \overline{H}_{int} = i\omega\mu_0 l^2(H_0 - FJ + J)$. The current in the metallic loop is equal to the displacement current in the gap formed by the top and bottom L-strips, we get $J = \frac{1}{h} d_c l \cdot \frac{d}{dt} D_2 = -i\omega l d_c \epsilon_d E_2/h = \frac{1}{h} d_c t_m \frac{d}{dt} D_1 = -i\omega d_c t_m \epsilon_m E_1/h$. Where ϵ_d is the permittivity of the dielectric substrate, and $\epsilon_m = \epsilon_0[1-\omega_p^2/(\omega^2+i\omega\gamma)] \approx -\epsilon_0\omega_0^2/(\omega^2+i\omega\gamma)$ is the permittivity of the metallic wire. We therefore get $E_1 = ih/(\omega t_m d_c \epsilon_m)J$, and $E_2 = ih/(\omega l d_c \epsilon_d)J$. From the emf equation, we can calculate the current density: $J = i\omega\mu_0 l^2 H_0/[-i\omega\mu_0 l^2(1 - F) + i4lh/(\omega d_c t_m \epsilon_m) + i4ht/(\omega l d_c \epsilon_d)]$. Finally we get the effective permeability of the split-ring resonator given by

$$\frac{\mu_{eff}}{\mu_0} = 1 - \frac{\omega^2 F L_g/(L_g + L_i)}{\omega^2 - \omega_0^2 + i\omega\Gamma} \tag{1}$$

where $\omega_0 = 1/\sqrt{(L_g + L_i)C}$ is the magnetic resonance, $L_g = \mu_0 l^2/h$ is the geometrical inductance, $L_i = 4l/(\epsilon_0 d_c t_m \omega_p^2)$ is an inertial inductance that arises from the finite electron mass in the metal, $C = \epsilon_d l d_c/4t$ is the total capacitance in the magnetic resonant loop, and $\Gamma = \gamma L_i/(L_g + L_i)$ represent the dissipative term. We see that the effective permeability follows a Lorentz dispersive model. For perfect conductor, $\Gamma = 0$, and it can be seen that within the frequency range $\omega_0 \leq \omega \leq \omega_0/\sqrt{[1 - FL_g/(L_g + L_i)]}$, the effective permeability is negative. Using the parameters shown in (*20*), a rough estimate of the magnetic resonant frequency of the structure is around 11 GHz. If we use a more accurate model to calculate the capacitative value between the gap (*22*) by taking the fringe electric field into account using a computer, we get a more accurate resonant value around 8 GHz, in good agreement with the experimental

results (*20*). The magnetic response of the split-ring resonator to H_x and H_z fields can be neglected, thus we get $\mu_{xx} = \mu_0$ and $\mu_{zz} = \mu_0$. The effective magnetic parameters tensor of the structure is therefore given by $\overline{\overline{\mu}} = diag[\mu_{\|} \quad \mu_{\perp} \quad \mu_{\|}]$, where $\mu_{\perp} = \mu_{eff}$ following a Lorentz dispersive model, and $\mu_{\|} = \mu_0$.

The effective negative permittivity behavior of the array of thin metallic wires has been analyzed in (*16*) by calculating the effective electron density and effective mass of the wire system. The final expression for the plasma frequency shows independent of the microscopic quantities such as the electron density and the electron drift velocity (*23*). Therefore we can recast the problem by calculating the capacitances and inductances in the wire medium (*24*). When an external electric field is applied along the wires, current will be induced. The currents will produce magnetic fields circling the thin wires. The distance between the two adjacent parallel wires is h. Since by symmetry there is a point of zero field in between the wires, we hence can estimate the magnetic field along the line between two wires to be $H(\rho) = \hat{\phi}\frac{I}{2\pi}(\frac{1}{\rho} - \frac{1}{h-\rho})$. The inductance of the thin wires is so large that prevents the change of the currents flowing in these wires. The electric field can thus be related to the flowing currents by $E = -i\omega LI + \sigma t_m d_c I$, where L is the total inductance per unit length and σ is the conductivity of the metal (*24*). By integrating the magnetic flux passing through a plane from the wire to the symmetric point between itself and the adjacent wire, we can calculate the inductance, $L = \Phi/I = \frac{\mu_0}{I}\int_{t_m/2}^{h/2} H(\rho)d\rho = \frac{\mu_0}{2\pi}\ln[\frac{h^2}{4t_m/2(h-t_m/2)}]$. As the current density per unit volume in the wire medium is defined by $J = \frac{I}{ha/\sqrt{2}}$, the polarization per unit volume in the wire medium can be obtained by $P = \frac{J}{-i\omega} = \frac{E}{-i\omega ha/\sqrt{2}(-i\omega L+\sigma t_m d_c)}$. Finally we get the effective permittivity of the wire medium in the limit of $t_m \ll h$,

$$\epsilon_{eff} = \epsilon_d[1 - \frac{\omega_p^2}{\omega^2 + i\omega\gamma}] \tag{2}$$

where $\omega_p^2 = \frac{2\sqrt{2}\pi c^2}{\epsilon_d ha\ln[h/(2t_m)]}$ and $\gamma = \frac{\sigma t_m d_c}{\ln[h/(2t_m)]}$. Below ω_p, the effective permittivity of the wire

medium is negative. We see that the electric response of the wire array follows a Drude dispersive model. The two dimensional wire array shown in Fig. 2(a) behaves like an isotropic low frequency plasma in the xz plane. Since the electrical response of the wire medium to E_y field can be neglected, the constitutive parameter tensor is therefore given by $\overline{\overline{\epsilon}} = diag[\epsilon_\parallel \quad \epsilon_\perp \quad \epsilon_\parallel]$, where $\epsilon_\parallel = \epsilon_{eff}$ following a Drude dispersive model, and $\epsilon_\perp = \epsilon_b$ is the dielectric constant of the background medium.

We can separate all field components into their y component and x, z components from the Maxwell equations (*9*). The two Maxwell equations for anisotropic medium become

$$\begin{aligned}(\overline{k}_s + \hat{y}k_y) \times (\overline{E}_s + \overline{E}_y) &= \omega(\mu_\parallel \overline{H}_s + \mu_\perp \overline{H}_y) \\ (\overline{k}_s + \hat{y}k_y) \times (\overline{H}_s + \overline{H}_y) &= -\omega(\epsilon_\parallel \overline{E}_s + \epsilon_\perp \overline{E}_y)\end{aligned} \tag{3}$$

where $\overline{k}_s = \hat{x}k_x + \hat{z}k_z$, $\overline{E}_s = \hat{x}E_x + \hat{z}E_z$, and $\overline{H}_s = \hat{x}H_x + \hat{z}H_z$. We therefore have

$$\begin{aligned}\overline{k}_s \times \overline{E}_s &= \omega\mu_\perp \overline{H}_y \\ \overline{k}_s \times \overline{E}_y + k_y(\hat{y} \times \overline{E}_s) &= \omega\mu_\parallel \overline{H}_s \\ \overline{k}_s \times \overline{H}_s &= -\omega\epsilon_\perp \overline{E}_y \\ \overline{k}_s \times \overline{H}_y + k_y(\hat{y} \times \overline{H}_s) &= -\omega\epsilon_\parallel \overline{E}_s.\end{aligned} \tag{4}$$

From these equations, we can express $\overline{E}_s$ and $\overline{H}_s$ in terms of E_y and H_y, and further we can obtain the following Helmholtz equations for E_y and H_y

$$\begin{aligned}\left[\omega^2\epsilon_\parallel - \frac{k_y^2}{\mu_\parallel} - \frac{k_s^2}{\mu_\perp}\right] H_y &= 0 \\ \left[\omega^2\mu_\parallel - \frac{k_y^2}{\epsilon_\parallel} - \frac{k_s^2}{\epsilon_\perp}\right] E_y &= 0.\end{aligned} \tag{5}$$

If the wave is propagating in the xz plane with $\overline{H}_y$ polarized field (TM case), *i.e.* $k_y = 0$, we get $[\omega^2\mu_\perp\epsilon_\parallel - k_s^2]H_y = 0$. We therefore see that in this simple case, the field depends on only the $\mu_\perp$ and $\epsilon_\parallel$ components. The original constitutive parameter tensors, which are 3×3 complex

matrix, is therefore diagonalized here. The Maxwell equations are reduced to the following two: $\overline{k}_s \times \overline{H}_y = -\omega\epsilon_{\|}\overline{E}_s$, and $\overline{k}_s \times \overline{E}_s = \omega\mu_{\perp}\overline{H}_y$. Note that $\mu_{\perp}$ and $\epsilon_{\|}$ follow Lorentz and Drude dispersive model respectively. For the lossless case in the overlapped frequency band where both of them are negative, the time averaged Poynting vector $\langle\overline{S}\rangle = \langle\overline{E}_s \times \overline{H}_y^*\rangle = \langle\overline{E}_s \times \frac{1}{\omega\mu_{\perp}^*}(\overline{k}_s \times \overline{E}_s)^*\rangle = \frac{|E_s|^2}{2\omega\mu_{\perp}}\overline{k}_s$, which is opposite to the wave vector k_s for a negative $\mu_{\perp}$, representing a backward propagating wave. It also shows that $\overline{E}_s$, $\overline{H}_y$, and $\overline{k}_s$ form a left-handed triad. The Helmholtz wave equation gives $k_s = \frac{\omega}{c}\sqrt{n}$, where $n = \pm\sqrt{\frac{\mu_{\perp}\epsilon_{\|}}{\mu_0\epsilon_0}}$. In order to determined the correct solution of the refractive index, we include slightly some loss into the permittivity and permeability. The imaginary parts of the permeability and permittivity are required to be positive for any passive medium, the relative complex values of the two parameters can be expressed as $\mu_r = \mu_{\perp}/\mu_0 = |\mu_r|e^{i(\pi-\delta_1)} = |\mu_r|(-\cos\delta_1 + i\sin\delta_1)$ and $\epsilon_r = \epsilon/\epsilon_0 = |\epsilon_r|e^{i(\pi-\delta_2)} = |\epsilon_r|(-\cos\delta_1 + i\sin\delta_1)$ with δ_1,$\delta_2 \ll 1$ and being positive. The refractive index of the medium is $n = \pm\sqrt{|\mu_r\epsilon_r|}[\cos(\frac{\delta_1+\delta_2}{2}) - i\sin(\frac{\delta_1+\delta_2}{2})]$. Since any passive medium requires the imaginary part of the refractive index to be positive, we therefore get a negative real part of the refractive index $n' = -\sqrt{|\mu_r\epsilon_r|}\cos(\frac{\delta_1+\delta_2}{2}) \approx -\sqrt{|\mu_r\epsilon_r|}$.

The negative refractive index of the constructed metamaterial has been proved by the prism experiment for transverse magnetic polarized incidence (Fig. 2(b)). It is demonstrated that the refractive index of the metamaterial is negative from 8.1 to 9.5 GHz. The unit cell of the metamaterial has a size of 3 mm, which is less than one tenth of the wavelength at the negative refraction region, i.e. 31$\sim$37 mm. The composite structure therefore can be considered as an effective homogenous left-handed medium.

With the presently available fabrication technology, it is possible to reach much higher frequencies by scaling down the corresponding length scales. However, metals may no longer behave as perfect conductors and electromagnetic fields may penetrate considerably into the metal when the structure is scaling to higher infrared and optical frequencies, which may deteriorate

the magnetic activity of the split-ring resonator. For example, for copper, $\omega_p \approx 1.6 \times 10^{16}$ Hz, $\gamma \approx 3.2 \times 10^{13}$ Hz. In several Gig Hz frequencies, the inertial inductance, $L_i = 6 \times 10^{-16}$ H, is almost seven orders of magnitude smaller than the geometrical inductance, $L_g = 2.5 \times 10^{-9}$ H, and can be neglected. However, if we scale the geometry size of our device by a factor of 1000 and thus the working frequency to several Tera Hz, then $L_i = 6 \times 10^{-13}$ H is comparable to $L_g = 2.5 \times 10^{-12}$ H. This will lead to three important effects when the geometry size scale down: Firstly, the magnetic resonance, $\omega_0 = 1/\sqrt{(L_g + L_i)C}$, will increase less than a factor of 1000 due to the presence of the inertia inductance takes effect in the higher frequencies. Secondly, the dissipative term $\Gamma = \gamma L_i/(L_g + L_i)$, which being 2 orders of magnitude smaller than the Gig Hz and thus negligible in the microwave frequencies, will increase to 6 THz comparable to the THz operating frequencies and hence deteriorate the magnetic resonance behavior. Thirdly, the effective fraction volume $FL_g/(L_g + L_i)$ decreases, indicating the relative bandwidth of the frequency band with negative permeability will decrease in the higher frequencies.

There can be many possible metamaterial designs for reversed Cherenkov radiation. In order to achieve a successful metamaterial design one should at least take the following issues into consideration: (1) The characteristic of the radiated electromagnetic waves from Cherenkov radiation requires that the components of $\mu_{\phi\phi}$, ϵ_{zz}, and $\epsilon_{\rho\rho}$ to be negative. Therefore the split-ring resonators and the metal wires should be in-plane, *i.e.* they may locate in the same substrate layer or in the top or bottom sides of the layer. The coupling between them might be increased and destroy their individual resonant behavior. A successful design should minimize this kind of coupling. For example, the metal wires shown in Fig. 2(a) cross over the center of the split-ring resonators without any contact. The incident electric field will induce currents flowing along the wires, which will in turn produce magnetic fields around the wires. However, these magnetic fields have zero net magnetic flux perpendicular to the split-ring resonator plane due to the symmetric pattern with respect to the wire, and therefore have little effect on the magnetic

behavior of the split-ring resonator. (2) Since Cherenkov radiation is faint, metamaterial with low loss is very important for a successful detection. In the microwave frequencies, the dielectric loss dominates, substrate with low loss can be used in the metamterial design. While in THz or optical frequency, the Omega loss may dominate, metal with low loss such as silver or even superconductors can be good candidate for the design. As dielectric loss is smaller compared with metallic loss in the optical frequency, some dielectric resonators with subwavelength resonant mode (*25, 26*) can also be used in metamaterial design for Cherenkov radiation. (3) Metamaterial for reversed Cherenkov radiation exhibits isotropic electrical response. The unit cell of the design therefore should have some kind of symmetry, such as rotational symmetry or rotoreflection symmetry.

Demonstration of Reversed Cherenkov Radiation

It is challenging to experimentally test the reversed Cherenkov radiation in the left-handed medium due to the following two reasons: First, the intensity of Cherenkov radiation increases with higher frequencies, indicating optical or ultraviolet spectrum are more suitable for detection. However, in order to realize metamaterial with effective negative permittivity and permeability at optical or ultraviolet frequencies, the unit size of the metamaterial should be much smaller than the wavelength (700 nm -10 nm). Although great effort has been devoted to push the working frequency of metamaterial from microwave to optical frequencies (*27*) in the past years, the technique of fabrication is still much less mature in optical frequencies, not to mention the loss increment in the metal as it scales to the optical spectrum. Second, to convincingly demonstrate reversed Cherenkov radiation in left-handed medium, the far field of the radiated waves needs to be measured, however, it is not practical to build a large block of left-handed medium and measure the far field inside of the metamaterial.

In an earlier work, Cherenkov radiation in a metamaterial-loaded waveguide with a charged

particle beam incidence was carried out in microwave frequency (*28*). Microwave radiation peak was observed at the left-handed band of the metamaterial, showing some evidence of Cherenkov radiation in the left-handed medium. Although backward Cherenkov radiation was not observed due to the beam fluctuations in this measured scheme in this study, it is the first experimental attempt to use charged particle beam to measure the Cherenkov radiation in metamaterial.

In order to convincingly demonstrate the backward Cherenkov radiation in left-handed medium, Xi *et al.* proposed the concept using a waveguide with an array of open slots to emulate a fast moving charged particle. With these setup, the problem of weak Cherenkov radiation from a charged particle in the microwave frequencies was side-stepped, enabling the verification of reversed Cherenkov radiation in the low frequency band (*20*). As a monochromatic microwave propagating in the slot waveguide, it emitted through each of the slots with a fixed phase delay relative to its neighboring slots because the input microwave take a longer time to travel to the more distant slots. The slot waveguide thus functions as a phased dipole array. By comparing the electric current carried by a moving charged particle with the current density of the slot waveguide in the frequency domain, it was shown that they are very similar except that the moving charged particle contains the whole spectrum of the frequencies while the slot waveguide has only one working frequency. As long as single frequency is concerned, the behavior of the moving charged particle and the phased dipole array are exactly the same. Therefore, the slot waveguide emulates a monochromatic Cherenkov source with its charged particle moving with a frequency-dependent speed. A prism-like sample is used for measurement instead of building a large block of left-handed medium. At the prism interface, the reversed Cherenkov wave gets refracted to a larger angle (negative refraction band) than the ordinary Cherenkov wave (positive refraction band), and can thus be distinguished from a forward Cherenkov wave (Fig. 3(a)). The measured far field pattern therefore successfully

demonstrates the reversed Cherenkov radiation in the left-handed medium (Fig. 3(b)).

If we look into the phase matching phenomena associated with the reversed Cherenkov radiation, we could further improve our understanding of the intrinsic connection between Cherenkov radiation and the refraction at the interfaces of two medium. It is pointed out that the charged particle beam (or the equivalent slot waveguide) can be viewed as a medium with a lower positive index of c/v_p, where v_p is the phase velocity of the particle (*29*). In the reversed/conventional Cherenkov radiation, the light is negatively/positively refracted from a lower positive index medium to a higher negative/positive index medium at a grazing incident angle. The refraction angle is $\sin^{-1}(\frac{c/v_p}{n})$, which is exactly complement to the angle of the Cherenkov cone: $\theta = \cos^{-1}(\frac{c/v_p}{n})$.

Perspective and Challenge

The unusual Cherenkov radiation in metamaterials opens a window for many new applications. The most important application is for particle identification. One could measure the velocity of an charged particle by the properties of the Cherenkov wave emitted in the left-handed medium. The mass of the particle can be computed and thus it can be identified if the momentum of the particle is measured independently. The Cherenkov radiation based on left-handed medium has a distinct advantage that the photon and charged particle are naturally separated in opposite directions so their physical interference is minimized.

Moreover, the left-handed metamaterial we have introduced is electrical isotropic only in two orthogonal directions. With further refinement, metamaterial can be made as isotropic, anisotropic, and bianisotropic. Many striking phenomena may be realized with such flexible constitutive parameters of the metamaterial. One interesting phenomenon is that Cherenkov radiation without any velocity threshold may be generated by utilizing anisotropic metamaterial. This unusual phenomenon has been previously observed in metallic grating (*30*) and photonic

crystals (*31*). Here metamterial provides an additional solution with more material flexibility. The radiation pattern covers a much larger angle from forward to backward, thus Cherenkov detector based on anisotropic metamaterial possess strong velocity sensitivity and good radiation directionality.

Finally, electromagnetic detection of perfect invisibility cloak becomes possible which rely much on the Cherenkov phenomena in metamaterial. The invisible cloak has received great interest recently (*32–38*). It is designed based on a transformation method, and relies on metamaterial to provide the specific constitutive parameters. Theoretical work show that the ideal cloak can be perfectly invisible from electromagentic waves (*38*). Since causality requires metamaterials for cloak to be dispersive, practical cloak can work only for a certain frequency band. However, a recent paper show that no matter the invisibility cloak works in any frequency band, it can still be electromagnetically detected by shooting a fast charged beam (*39*). A broad band Cherenkov wave will be radiated out as the particle travels through the cloak, making the cloak visible. The reason is due to the fact that photon cannot perceive a transformed (or curved) electromagnetic space while the moving particle can perceive the transformed electromagnetic space because the mechanical space governed by the Newton's laws of motion is still flat. Concretely, a spherical cloak is a transformed electromagnetic space (or physical space, see Fig. 4(a)) created by squeezing the virtual flat electromagnetic space (or free space, see Fig. 4(b)) such that a hole in the physical space is generated. In the physical space, photons (or the light rays) are bent around the concealed region to make the cloak invisible, while in a flat electromagnetic space, the trajectory of the photons is a line. Photons cannot perceive whether the electromagnetic space is curved or not when propagation. However, the charged particle, which moves uniformly along a straight line in the physical space, will move nonuniformly in the virtual electromagnetic space (*39*). The trajectory of the particle will be bent (Fig. 4(b)). The velocity of the particle can be larger than the speed of light in the virtual electromagnetic space

and generate radiation (Fig. 4(c)). The implication from this study is enormous. The combination of transformation metamaterial with Cherenkov radiation makes a host of new physical phenomena and applications possible, many of which were unthinkable in the past. While we are very familiar with the fact that the explanation of Cherenkov radiation phenomena owes to Frank and Tamm (*2*), we may less know that Sommerfeld has already submitted the hypothetical case of the movement of an electron at a speed greater than that of light in a vacuum to a theoretical study in 1904 to 1905 (*40*), shortly before the theory of relativity came into being. It is very unlucky to Sommerfeld that the coming of the theory of relativity by Einstein who affirms that material bodies are unable to move at the speed of light, overshadowed Sommerfeld's conclusions which seemed less to the purpose. However, by utilizing the transformed metamaterial, we can realize an equivalent virtual electromagnetic space where the speed of the charged particle in the virtual electromagnetic space can exceed the light, allowing the Cherenkov radiation to occur both in the virtual electromagnetic space and in the physical space. Cherenkov radiation in the left-handed medium therefore can also be viewed as a radiation phenomena when a charged particle moving in a virtual negative electromagnetic space. We therefore can flexibly manipulate the Cherenkov photons by constructing the metamaterial with specific parameters to mimic the virtual electromagnetic space, which have potential applications in high energy physics, astrophysics, and novel radiation sources.

As a first step, the experimental work shown in (*20*) has demonstrated the manipulation of Cherenkov photon is possible in left-handed medium. Future work will be on direct demonstration of reversed Cherenkov radiation using actual moving charged particles, which is very important for practical applications. Due to the faint radiation field of the charged particle, achieving low loss metamaterial working in optical or even ultraviolet spectrum is full of challenge. Low loss metamaterial has an additional advantage that the sharp resonance allows the negative refractive index easily to be smaller than -1, which is a sufficient condition to ob-

serve backward Cherenkov radiation in isotropic left-handed medium. Another challenge to address for the development of devices based on reversed Cherenkov radiation is to improve the two-dimensional layered optical metamaterial to three-dimensional metamaterial. The recently achieved three dimensional optical metamaterial (*41*) offered the possibility to explore variety of the optical phenomena in this topic.

Conclusion

Metamaterials have shown great potential as artificial atoms with unusual electromagnetic properties, allowing a lot of new application become possible, such as perfect lens, invisibility cloaking, and reversed Cherenkov radiation. With the transformation optics method, metamaterials with specific parameters could mimic virtual electromagnetic space, and further control the motion of the charged particle in the virtual electromagnetic space, offering great flexibility to manipulate the Cherenkov photon. It offers new physics, new phenomena, and may lead to innovation in Particle Physics, Astrophysics, and Biomolecules, with the capability of their flexible parameters.

References and Notes

1. P. A. Cerenkov, *Dokl. Akad. Nau* **2**, 451 (1934).

2. I. M. Frank, I. E. Tamm, *Dokl. Akad. Nau* **14**, 107 (1937).

3. O. Chamberlain, E. Segre, C. Wiegand, T. Ypsilantis, *Phys. Rev.* **100**, 947 (1955).

4. J. J. Aubert *et al.*, *Phys. Rev. Lett.* **33**, 1404 (1974).

5. V. G. Veselago, *Sov. Phys. Usp.* **10**, 509 (1968).

6. J. B. Pendry, D. R. Smith, *Phys. Today* **57**, 37 (2004).

7. J. B. Pendry, *Science* **322**, 71 (2008).

8. D. R. Smith, J. B. Pendry, M. C. K. Wiltshire, *Science* **305**, 788 (2004).

9. J. A. Kong, *Electromagnetic Wave Theory* (EMW Publishing, Cambridge, MA, 2005).

10. J. D. Jackson, *Classical Electrodynamics* (John Wiley and Sons, New York, 1999).

11. H. Minkowski, *Natches. Ges. Wiss. Gottingen* **53**, (1908).

12. J. Lu *et al.*, *Opt. Express* **11**, 723 (2003).

13. T. Musha, *Proceedings of the IEEE* **60**, 12 (1972).

14. M. Abraham, *Rend. Circ. Mat. Palermo* **28**, 1 (1909).

15. B. A. Kemp, J. A. Kong, T. M. Grzegorczyk, *Phys. Rev. A* **75**, 053812 (2007).

16. J. B. Pendry, A. J. Holden, W. J. Stewart, I. Youngs, *Phys. Rev. Lett.* **76**, 4773 (1996).

17. J. B. Pendry, A. J. Holden, D. J. Robbins, W. J. Stewart, *IEEE Trans. Microwave Theory Tech.* **47**, 2075 (1999).

18. D. R. Smith, W. J. Padilla, D. C. Vier, S. C. Nemat-Nasser, S. Schultz, *Phys. Rev. Lett.* **84**, 18 (2000).

19. R. A. Shelby, D. R. Smith, S. Schultz, *Science* **292**, 77 (2001).

20. S. Xi *et al.*, *Phys. Rev. Lett.* **103**, 194801 (2009).

21. S. O'Brien, J. B. Pendry, *J. Phys: Condens. Matter* **14**, 6383 (2002).

22. C. P. Yuan, T. N. Trick, *IEEE Electron Device Lett.* **3**, 391 (1982).

23. S. A. Ramakrishna, *Rep. Prog. Phys.* **68**, 449 (2005).

24. S. I. Maslovsky, S. A. Tretyakov, P. A. Belov, *Microwave Opt. Tech. Lett.* **35**, 47 (2002).

25. S. O'Brien, J. B. Pendry, *J. Phys: Condens. Matter* **14**, 4035 (2002).

26. L. Peng *et al.*, *Phys. Rev. Lett.* **98**, 157403 (2007).

27. V. M. Shalaev, *Nature Photonics* **1**, 41 (2007).

28. S. Antipov, *et al.*, *J. Appl. Phys.* **104**, 014901 (2008).

29. S. Zhang, X. Zhang, *Physics* **2**, 91 (2009).

30. S. J. Smith, E. M. Purcell, *Phys. Rev.* **92**, 1069 (1953).

31. C. Luo, M. Ibanescu, S. G. Johnson, J. D. Joannopoulos, *Science* **299**, 368 (2003).

32. J. B. Pendry, D. Schurig, and D. R. Smith, *Science* **312**, 1780 (2006).

33. U. Leonhardt, *Science* **312**, 1777 (2006).

34. D. Schurig *et al.*, *Science* **314**, 977 (2006).

35. R. Liu *et al.*, *Science* **323**, 366 (2009).

36. J. Valentine, J. Li, T. Zentgraf, G. Bartal, X. Zhang, *Nature Mater.* **8**, 568 (2009).

37. L. H. Gabrielli, J. Cardenas, C. B. Poitras, M. Lipson, *Nature Photonics.* **3**, 461 (2009).

38. H. Chen, B.-I. Wu, B. Zhang, J. A. Kong, *Phys. Rev. Lett.* **99**, 063903 (2007).

39. B. Zhang, B.-I. Wu, *Phys. Rev. Lett.* **103**, 243901 (2009).

40. A. Sommerfeld, *Gottingen Nachr.* **99**, (1904).

41. J. Valentine *et al.*, *Nature* **455**, 376 (2008).

42. Supported by the Office of Naval Research under Contract No. N00014-06-1-0001, the Department of the Air Force under Contract No. FA8721-05-C-0002, the NNSFC (60801005, 60990320, and 60990322), the FANEDD (200950), the ZJNSF (R1080320), and the Ph.D Programs Foundation of MEC (200803351025).

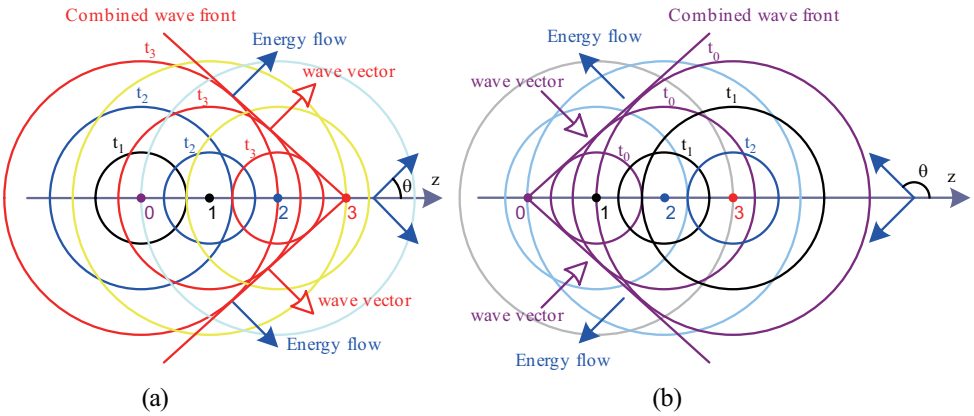

Figure 1: The geometry of (a) Cherenkov radiation and (b) reversed Cherenkov radiation.

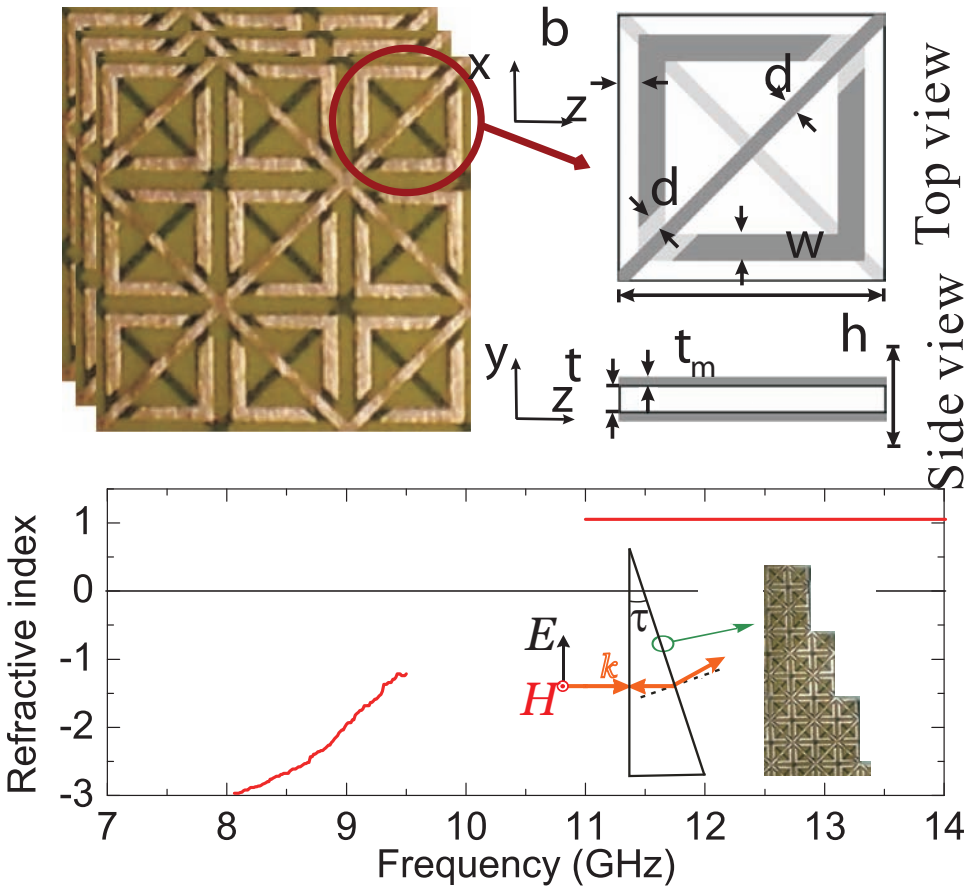

Figure 2: (a) Configuration of the metamaterial for reversed Cherenkov radiation (b) The measured refractive index of the metamaterial for transverse magnetic polarized field incidence.[Adapted from (*20*)]

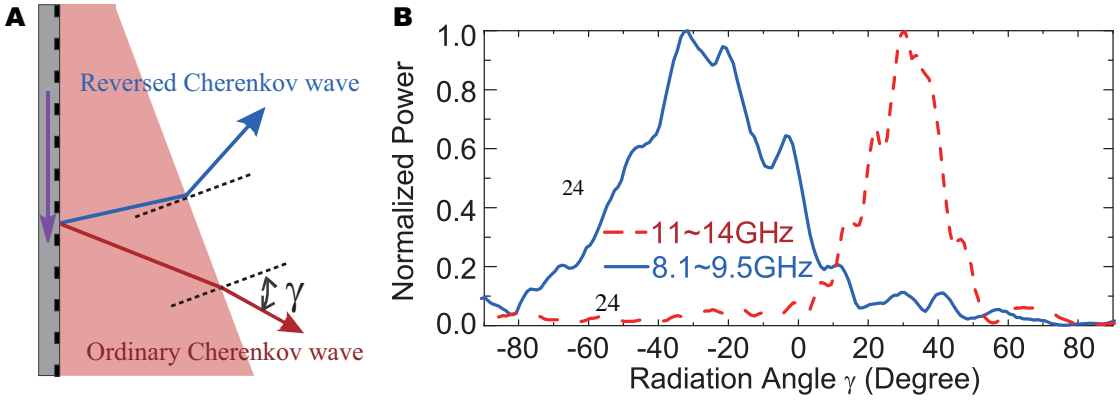

Figure 3: (a) Experimental setup to demonstrate reversed Cherenkov radiation. A slot waveguide is used to model a fast charged particle. The prism-like metamaterial is used to filter the Reversed Cherenkov wave. (b) Sum of the radiation power in each angle in the negative refraction band and positive refraction band.[Adapted from (*20*)]

This image has been removed due to copyright restrictions. Please see Figure 1 and Figure 2 on http://prl.aps.org/pdf/PRL/v103/i24/e243901.

MIT OpenCourseWare
http://ocw.mit.edu

8.07 Electromagnetism II
Fall 2012

For information about citing these materials or our Terms of Use, visit: http://ocw.mit.edu/terms.